Proceedings of the 2001 IEEE
International Conference on Robotics & Automation
Seoul, Korea • May 21-26, 2001

DYNAMIC COMPLIANT QUADRUPED WALKING

Martin de Lasa
Dept. of Electrical Engineering

Martin Buehler
Dept. of Mechanical Engineering

Centre for Intelligent Machines, McGill University, Montréal, Québec H3A 2A7
mdelasa|buehler@cim.mcgill.ca

Abstract

This paper presents a new dynamic walking controllers for quadrupedal robots with compliant legs. The algorithm implements a "walking bound" gait, (running bound without flight phase), requires only one actuator per leg at the hip, and commands a constant hip velocity during stance. The algorithm has been implemented successfully on our *Scout II* quadruped robot and has yielded stable walking for ranges of operating conditions with minimal reliance on feedback. The experimental data is used to illustrate important considerations on torque generation that need to be taken into account both for successful implementations and realistic modeling of legged robots. In addition, we quantify the energetics of our walking experiments via the specific resistance and document dramatic differences between mechanical and electrical power.

1 Introduction

To date most legged robotics research has focused on the study and implementation of systems with many actuated degrees of freedom. This has often yielded robots whose full range of motion was difficult to exploit, due to high system complexity, high weight, and to a lack of formal methods for the development of robust control schemes.

To investigate the potential of low actuated degree of freedom legged platforms, a walking algorithm for an underactuated compliant legged quadrupedal robot, *Scout II*, built at McGill University's Ambulatory Robotics Lab (ARL), was developed. Each of Scout II's legs has one actuated rotational hip joint and a passive prismatic joint. Since Scout II does not have knees, the walk and trot gaits observed in nature are not currently realisable. Instead a version of the bound, called a walking bound, was investigated that differed from the running bound observed in nature since the robot was never ballistic during a locomotion stride.

Studying simple legged robotic platforms has several advantages: i) Dominant dynamic factors influencing locomotion can be determined ii) Locomotion energetics can help identify crucial or redundant actuators, iii) Systems can be designed with complexity added incrementally, iv) A practical body of control techniques and theory can be developed.

The reduction in system complexity resulting from a straightforward robot design also achieves another, perhaps more important, goal: Cost is lowered and reliability is increased while achieving mobility sufficient for many robotic task domains. We believe that these characteristics will help bring legged robots out of the research lab and into the real world.

Despite these many advantages, underactuated robots impose significant restrictions on designers of locomotion algorithms by limiting control inputs. Further constraints arise since the need for untethered operation dictates that actuator weight must be kept low forcing actuators to be used in peak power regions, where available torque is highly dependent on velocity. Slip between the toe and the ground further limits deliverable torque.

2 Background

With the exception of [1], little work exists on dynamical walking controller design for underactuated quadruped robots. However, closely related work exists in three areas: control of dynamic running robots, control of dynamic walking robots with articulated legs, and legged robot control exploiting passive dynamics.

In the area of control of dynamic running robots, Raibert [2] proposed a novel three part running controller for one, two, and four legged robots using powerful hydraulic actuators. To improve upon the

0-7803-6475-9/01/$10.00 © 2001 IEEE

robot energetics Gregorio [3], and Ahmadi[4] designed electric versions of Raibert's one-legged hopper, Monopods I and II, reducing mechanical power to less than 68 W. More recently, Papadopoulos and Buehler [5] obtained stable open-loop quadrupedal pronking and bounding, at speeds of up to 1.2 m/s, using a modified version of the three-part algorithm, torque control in stance, and a quasi-static slip control algorithm, despite a robot design without linear leg actuation.

In the area of control development for robots with articulated legs, Dunn and Howe [6] proposed a dynamic bipedal walking controller that constrained touchdown hip velocity. Pratt [7] proposed another technique, *Virtual Model Control*, later used in [8]. Others [9, 10], have turned toward the concept of *Zero Moment Point* (ZMP) to avoid the postural instability resulting from foot rotation during bipedal walking. Biologically inspired methods of legged robot control have also been used by Taga [11] and Kimura [12] in simulation and experiment respectively.

In the area of robot control exploiting passive system dynamics, McGeer [13], built a series of bipeds capable of walking passively down shallow inclines powered only by gravity. Ringrose [14] showed that using (roughly) semi-circular feet stable dynamic running could be acheived despite lack of sensor feedback. Similarly, Buehler et al. [15, 16] showed that using a simple robot design having only one actuated degree of freedom per joint, stable open-loop walking, turning, and step climbing could be acheived. Their Scout I and Scout II robots, used stiff stick legs and relied on momentum transfer to maintain regular body pitching.

3 Experiment

Preliminary experiments [1] revealed that front and back sets of legs play markedly different roles in quadrupedal walking. In contrast to the back legs that provide bulk forward propulsion for locomotion, the front legs act as brakes slowing the forward motion of the body and helping to lift the back legs off the ground. Given this antagonist relationship, a simple open loop walking controller was devised that swept the back legs at a constant hip velocity, matching the desired forward speed of the center of mass (COM), and that kept the front legs at a user specified touchdown angle. This approach proved stable in experiments, but was very sensitive to changes in both walking surface and controller parameters. To improve upon these characteristics a few refinements were made to the previously devised controller. Figure 1 shows a planar model of Scout II used to develop the described walking controller. Table 1 summarizes controller actions. As with the previous controller,

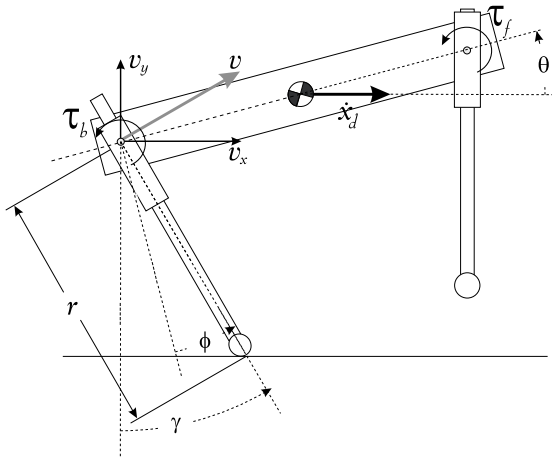

Figure 1: Planar scout ii controller model showing key nomenclature.

two indepedent state machines were used to control the behaviour of front and back pairs legs. Each state machine switched between *flight* and *stance* depending on the state of a virtual leg formed by grouping left and right legs at each hip. During flight, both front and back pairs of legs were servoed to a desired touchdown angle, $\gamma_{d\,td\,f}$ and $\gamma_{d\,td\,b}$ respectively. In stance, the back legs were commanded to sweep backwards, tracking the user specified horizontal hip velocity $\dot{x}_d$. Similarly, during stance, the front legs were commanded to track a fraction of the desired back leg speed determined by $\dot{x}_{ratio}$. A heuristical search of the

Table 1: Open loop constant hip velocity controller.

Legs	State	Action
Front	Stance	$\gamma_{d\,i} = \int \dot{\gamma}_{d\,i}\, dt$
		$\dot{\gamma}_{d\,i} = \frac{\dot{x}_d}{r_i(t)\, cos(\gamma_i(t))}\, \dot{x}_{ratio}$
	Flight	$\gamma_{d\,i} = \gamma_{d\,td\,f}$
		$\dot{\gamma}_{d\,i} = 0$
Back	Stance	$\gamma_{d\,i} = \int \dot{\gamma}_{d\,i}\, dt$
		$\dot{\gamma}_{d\,i} = \frac{\dot{x}_d}{r_i(t)\, cos(\gamma_i(t))}$
	Flight	$\gamma_{d\,i} = \gamma_{d\,td\,b}$
		$\dot{\gamma}_{d\,i} = 0$

parameter space revealed stable open loop behaviour for $\gamma_{dtdf} = 0^o$, $\gamma_{dtdb} = 26^o$, $\dot{x}_d = 0.2\ m/s$, and $\dot{x}_{ratio} = 15\ \%$. A high gain *proportional derivative* (PD) servo was used to calculate torque to command to each motor.

3.1 Experimental Results

Experiments with the proposed controller yielded stable walking, despite an open loop strategy that used two decoupled state machines. Figure 2 shows snapshots from a typical locomotion stride. Experimental results for another experiment are shown in figure 3.

As can be observed from figure 3, the body pitches

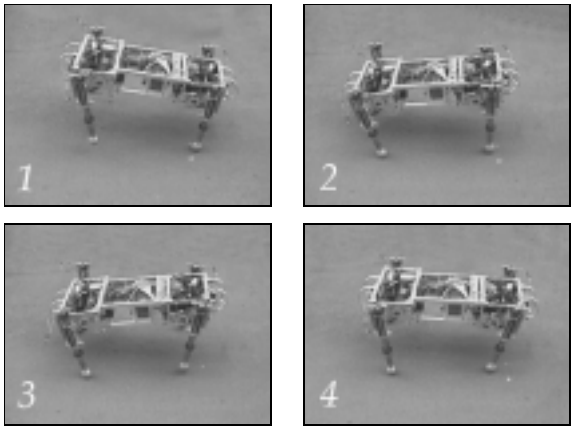

Figure 2: Key frames of Scout II in a bounding walk. Four distinct phases are observable : 1) Single Support (Back), 2) Double Support (Back to Front), 3) Single Support (Front), and 4) Double Support (Front to Back)

repeatably with a peak to peak amplitude of approximately 15^o at a frequency of $1.5\,Hz$. Mean perpendicular ground/toe clearances for the front and back toes are of 0.015 and $0.06\,m$. Figure 3 also shows the previously mentioned antagonistic behaviour of the front and back legs.

During stance, the front legs can be observed applying mostly positive torque, acting to brake the body, while the back legs apply negative torque propelling the body forward. Considerable tracking error can be observed in the back leg trajectory tracking, partly due to the large impacts during state transitions from flight to stance. Further sources of tracking error are discussed in section 3.2.

Errors in forward velocity tracking also exist. Although we are commanding the back legs to track $\dot{x}_d = 0.2\,m/s$, the mean forward velocity of the COM

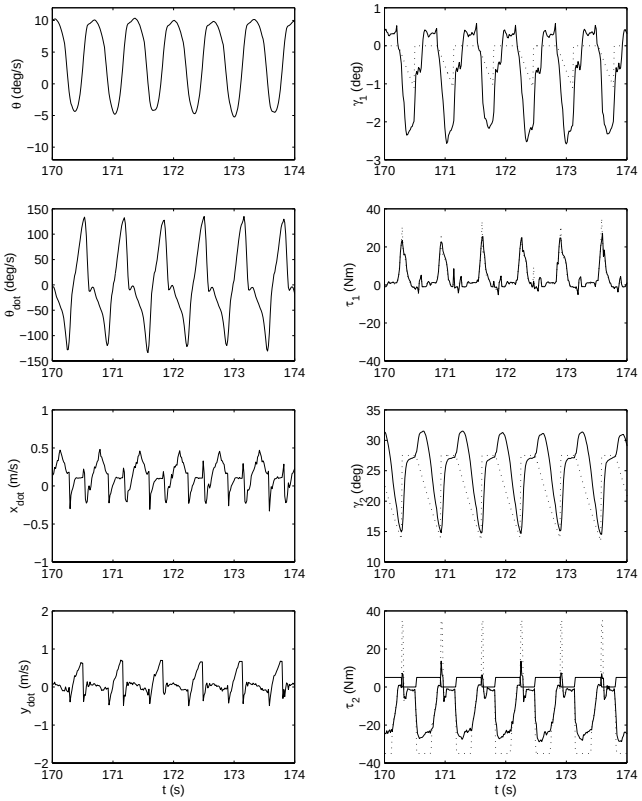

Figure 3: Experimental data from constant hip velocity walk: Presented velocity estimates calculated using kinematics.

was closer to $0.128\,m/s$ (calculated offline from data shown in figure 3). These errors can be explained by examining differences between commanded and actual front leg trajectories. Although the front legs are commanded to sweep in stance, they only move about 2.5^o, with approximately half of the deflection resulting from poor tracking. These errors are a consequence of the significant impacts experienced by the front legs at touchdown and from belt backlash in Scout's actuation system. Given this minor front leg displacement, the front legs can be thought of as remaining fixed throughout the stride. The sharp deccelerations in forward velocity, contribute to lifting the robot's hind legs off the ground, at the expense of producing large variations in forward velocity.

Experiments also revealed some unforseen system dynamics. Specifically, the back leg deflection behaviour did not match the expected parabolic profile for a spring mass system sliding in a frictionless slot, suggesting the presence of significant coulomb friction in the current leg design.

Despite these controller characteristics, the proposed dynamic compliant walking algorithm proved quite stable converging quickly to steady state walking. Variations in terrain slope and ground friction, had minor yet observable effects on controller performance.

3.2 Actuator Limits

The differences between commanded and applied motor torques in figure 3 provides some insight into the serious design constraints faced by developers of legged robots. Given Scout's requirements for autonomous operation, we must use light-weight motors (four brushed Maxon 90 W DC motors, run at 24 V, current limited to 12 A) in peak power regions, where the maximum achievable torque is highly limited by motor shaft velocity as shown in figure 4, by

$$\tau = \frac{K_T}{R_A} \left(V_T - K_\omega \, \omega\right) \tag{1}$$

where K_T is the torque constant, R_A is the armature resistance, K_ω is the back emf constant, ω is the shaft speed, and V_T denotes the maximum motor terminal voltage (in our case the robot's battery voltage). This torque limitation is also the cause of the difference between the desired torque (dashed dot line) and the torque calculated via the above torque speed limit (dotted line) in figure 5b.

It is interesting to note that there is still a discrepancy between the experimental torque speed data points in figure 4 which do not touch the polygonal limits. Similarly, in figure 5b the torque limit, calculated from (1) does still not match the actual torque measured. The reason is that the supply voltage to the motor, provided by the battery, varies itself as a function of current, due to the battery's internal resistance, R_A, as shown in figure 5a. This further reduces the available torque with increasing speed as follows: If we replace V_T with $V_{bat} - R_A * I = V_{bat} - R_A * \tau / K_T$ in (1) and solve for τ, we obtain a modified torque speed limit, which takes the voltage drop of figure 5a into account,

$$\tau = \frac{K_T}{R_A \alpha} \left(V_{bat} - K_\omega \, \omega\right) \tag{2}$$

where $\alpha = \left(1 + \frac{R_{bat}}{R_A}\right)$. This adjusted torque/speed limit (2) now provides an excellent match with the experimental torque data (dashed and solid lines in figure 5b).

Clearly understanding these torque limitations are of critical importance in designing legged robots. In addition, simulations need to be based on realistic models of torque production as described above in order to be useful.

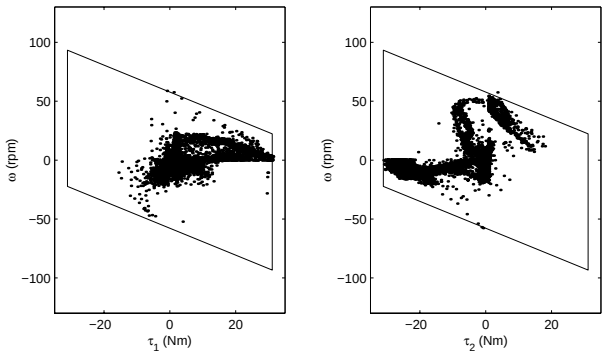

Figure 4: Front and back leg applied leg torque vs. leg speed : Experiment. The motor torque/speed limit polygon is also shown

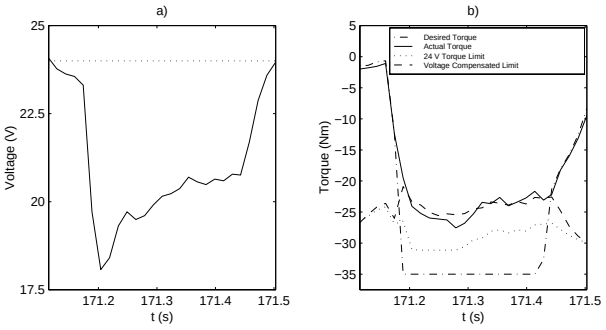

Figure 5: a) Supply voltage during a walking stride. b) Actual (solid), desired (dash-dot), 24 V limit, and voltage compensated torques for a walking stride : Experiment

3.3 Open Loop Controller Stability

To test controller stability an experiment was conducted in which the robot walking procedure was started under three different conditions: i) normal startup procedure, ii) startup from a large negative angle (-30^o), and iii) startup from a large positive angle (30^o). For all three vastly different startup conditions, the maximum body pitch of the robot (θ_{max}) converged back to the nominal walking values within three strides (see figure 6).

These results validate the stability of the open loop walking controller, however, they are also not entirely surprising given our previous observations of lossy leg

dynamics. Since the passive unforced system response is almost completely attenuated, convergence is almost entirely dependent on the energy added to the system by the controller.

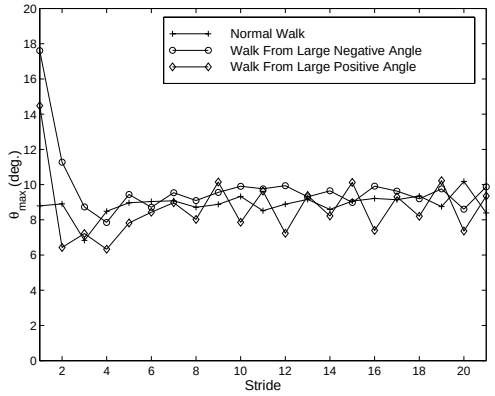

Figure 6: Open loop controller stability test results: Experiment.

3.4 Walking Energetics

One of the motivations for the study of underactuated legged robots is that reducing actuated degrees of freedom and exploiting passive dynamical system behaviour can lead to substantial energy savings. To objectively compare energy consumption of various systems (both legged and wheeled) Gabrielli and von Kármán [17] proposed a measure of locomotion energetics, called *specific resistance* (ε),

$$\varepsilon(v) \quad = \quad \frac{P(v)}{m\,g\,v}. \qquad (3)$$

Recently Gregorio and Buehler [3] presented a comparative study of the specific resistance of animals, wheeled, and legged vehicles/robots. Their findings showed large discrepancies in the literature with respect to how output power was measured. Although most robotics researchers use mechanical power when evaluating system power consumption, we believe that a more realistic measure of system energetics should be based on electrical power (to account for significant sources of loss such as heat dissipation, etc.).

As touched upon, both battery voltage and current deviate significantly from nominal steady state values during robot operation. Figure 7 shows the electrical and mechanical power calculated during walking, $P_e = V\,I$ and $P_m = \sum_{i=1}^{4} \mid \tau_i\,\dot{\phi}_i \mid$ respectively.

As anticipated the difference between input electrical power and output mechanical power is significant. For a mean input power of 234 W output mechanical power is 23 W. To obtain an estimate of specific resistance for Scout II, data from 10 walking experiments was gathered, for velocities ranging from $0.09 - 0.15\ m/s$. Average velocity, as well as electrical and mechanical power consumption for each of these experiments was calculated. Plotted estimates

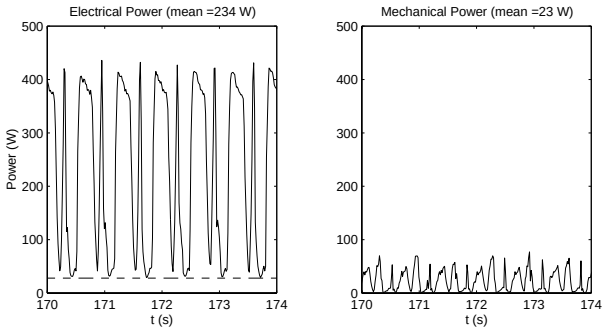

Figure 7: Electrical and mechanical power for 4 second open loop walk: Experiment. 28 W steady state electrical power indicated by dashed line in left plot.

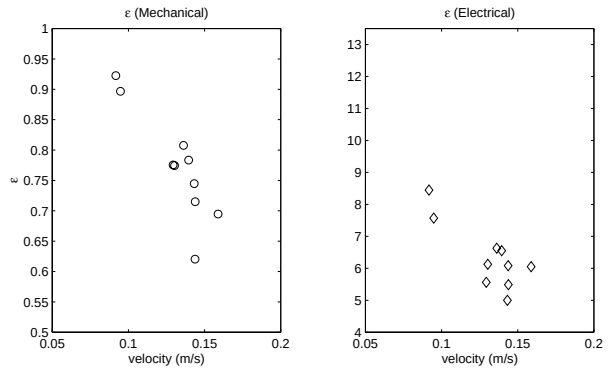

Figure 8: Mechanical and electrical specific resistance for a set of 10 experimental runs.

of ε using mechanical power in figure 8 yield specific resistance values as low as those for Monopod II (0.7) [4], even though few passive dynamical effects are currently being exploited on Scout II.

4 Conclusion

This paper presented a dynamic compliant walking algorithm for the Scout II robot, that used a simple open loop control strategy : constant hip velocity was commanded during periods of leg stance and legs were commanded to a fixed touchdown angle in flight.

The success of this simple controller parallels previous findings at ARL, showing that complex behaviours can be achieved using simple control strategies. Understanding the limits of this approach is the first step in producing truely useful and versatile robots.

We found that mechanical complexity is not a requisite for a walking robot. This said, it is unlikely that a single robot will accomodate all gaits with the same energetic efficiency. In the future, Scout's walking gait could be much improved with the redesign of the robot's legs, to take full advantage of the system's unforced response. In particular, reducing friction in the prismatic joints would help make both walking and running more efficient. Having found the significant effect variations in supply voltage can have on motor torque/speed limitations and on the controller effectiveness, future work should use more conservative estimates of achievable torque, both in simulation and experiment. This should not only help to bring simulation and experimental results in tighter correspondence with one another, but also help to further improve efficiency.

Acknowledgements

The authors would like to thank IRIS, a Federal Network of Centres of Excellence, and the Natural Science and Engineering Research Council of Canada for their support of this work. Don Campbell and Shervin Talebi also helped through much of this work.

References

[1] M. de Lasa and M. Buehler. Dynamic compliant walking of the scout ii quadruped: Preliminary experiments. *Proc. Int. Conf. Climbing and Walking Robots*, 2000.

[2] M. H. Raibert. *Legged Robots That Balance*. MIT Press, 1986.

[3] P. Gregorio, M. Ahmadi, and M. Buehler. Design, control, and energetics of an electrically actuated legged robot. *IEEE Trans. Systems, Man, and Cybernetics*, 27B(4):626–634, 1997.

[4] M. Ahmadi and M. Buehler. The arl monopod ii running robot: Control and energetics. *Proc. IEEE Int. Conf. Robotics and Automation*, pages 1689–1694, 1999.

[5] D. Papadopoulos and M. Buehler. Stable running in a quadruped robot with compliant legs. *Proc. IEEE Int. Conf. Robotics and Automation*, pages 444–449, 2000.

[6] E. R. Dunn and R. D. Howe. Towards smooth bipedal walking. In *Proc. IEEE Int. Conf. Robotics and Automation*, pages 2489–2494, 1994.

[7] J. E. Pratt, P. Dilworth, and G. A. Pratt. Virtual model control of a bipedal walking robot. In *Proc. IEEE Int. Conf. Robotics and Automation*, pages 193–198, 1997.

[8] C. M. Chew, J. E. Pratt, and G. A. Pratt. Blind walking of a planar bipedal robot on sloped terrain. In *Proc. IEEE Int. Conf. Robotics and Automation*, 1999.

[9] M. Vukobratović and D. Juricic. Contributions to the synthesis of biped gait. *IEEE Trans. Biom. Eng.*, BME-16:1–6, 1969.

[10] Hirai et al. The development of Honda humanoid robot. In *Proc. IEEE Int. Conf. Robotics and Automation*, pages 1321–1326, 1998.

[11] G. Taga, Y. Yamaguchi, and H. Shimizu. Self-organized control of bipedal locomotion by neural oscillators in unpredictable environment. *Biological Cybernetics*, 65:147–159, 1991.

[12] H. Kimura and Y. Fukuoka. Adaptive dynamic walking of the quadruped on irregular terrain - autonomous adaptation using neural system model. In *Proc. IEEE Int. Conf. Robotics and Automation*, pages 436–443, 2000.

[13] T. McGeer. Passive dynamic walking. *Int. J. Robotics Research*, 9(2):62–82, 1990.

[14] R. Ringrose. Self-stabilizing running. In *Proc. IEEE Int. Conf. Robotics and Automation*, 1997.

[15] M. Buehler et al. Scout: A simple quadruped that walks, climbs, and runs. *Proc. IEEE Int. Conf. Robotics and Automation*, pages 1701–1712, 1998.

[16] M. Buehler et al. Stable open loop walking in quadruped robots with stiff legs. *Proc. IEEE Int. Conf. Robotics and Automation*, pages 2348–2353, May 1999.

[17] G. Gabrielli and T. H. von Karman. What price speed ? *Mechanical Engineering*, 72(10):775–781, 1950.